AIAA JOURNAL
Vol. 51, No. 3, March 2013

Acoustic Velocity Formulation for Sources in Arbitrary Motion

G. Ghorbaniasl*
Vrije Universiteit Brussel, Brussels 1050, Belgium
M. Carley†
University of Bath, Bath, England BA2 7AY, United Kingdom
and
C. Lacor‡
Vrije Universiteit Brussel, Brussels 1050, Belgium

DOI: 10.2514/1.J051958

This paper deals with the acoustic velocity field simulation generated by interaction of flow with moving bodies. Starting from the Ffowcs Williams and Hawkings equation, an analytical formulation of the acoustic velocity is derived for sources in arbitrary motion. This makes the imposition of the boundary condition on a (rigid) scattering surface much more straightforward, as, if the traditional pressure formulation is used, then the pressure gradient must be calculated. Computational results for a pulsating sphere, dipole source, and a propeller case with subsonic tips verify this formulation.

Nomenclature

a_i'	=	acoustic velocity components
c_0	=	ambient speed of sound
f	=	data surface function
G	=	Green's function
g	=	retarded time function
L_i	=	loading source term
M_i	=	source Mach number components
$\hat{n}_i$	=	surface unit normal components
p	=	pressure
p'	=	acoustic pressure
Q	=	thickness source term
q	=	source term
r	=	distance between observer and source
$\hat{r}_i$	=	radiation direction unit
S	=	data surface area
t	=	observer time
u_i	=	flow velocity
v_i	=	data surface velocity
x_i	=	observer position
y_i	=	source position
β	=	angle of observer
δ	=	Dirac delta function
ρ	=	flow density
ρ_0	=	undisturbed flow density
τ	=	emission time variable

I. Introduction

THE ability to predict the velocity components of a sound wave radiated by a solid object in a fluid flow is one of the most significant goals in computational aeroacoustics. The need for acoustic velocity prediction exists in a wide range of aeroacoustic applications dealing with acoustic scattering problems, such as noise scattering by fuselage and wings in aircraft and noise scattering in rotating machines [1,2]. The various methods (for instance, [3]) for the solution of noise scattering problems require the acoustic velocity evaluation on the scattering surface. The evaluation of the acoustic velocity on the scattering surface is required in order to meet the boundary conditions (for instance, [4,5]). So far, the acoustic velocity has been evaluated using the acoustic pressure gradient through the linearized momentum equation. A direct numerical evaluation of the pressure gradient can be expensive for realistic cases. Recently, Lee et al. [6] have developed an efficient analytical formulation for the calculation of the acoustic pressure gradient. This formulation, which is referred to as formulation G1A, reduces the computational effort for the pressure gradient calculation. However, this formulation is somewhat complicated, and an indirect tool for acoustic velocity calculation. The present work is oriented to the development of an alternative, computationally efficient formulation, which determines the acoustic velocity directly.

In this paper, an analytical formulation of the acoustic velocity prediction is developed for sources in arbitrary motion. Starting from the Ffowcs Williams and Hawkings (FW-H) equation [7] with a penetrable data surface (FW-H_{pds}), and following the procedure used by Farassat for the derivation of formulations 1 and 1A [8,9], the acoustic velocity formulation is developed in the time domain. The derived formulation uses the flowfield data on the data surface enclosing the moving body and predicts the acoustic velocity field for an observer fixed to a medium at rest. This analytical formulation makes the imposition of the boundary condition on a (rigid) scattering surface much more straightforward, as, if the traditional pressure formulation is used, then the pressure gradient must be calculated.

It will be demonstrated that the developed formulation is significantly simpler than formulation G1A. Furthermore, this formulation is much easier to implement and requires fewer numerical operations than formulation G1A. Computational results for a pulsating sphere, a three-dimensional dipole source, and a conventional helicopter blade case with subsonic tips verify the derived formulation.

The layout of this paper is as follows: In Sec. II, the mathematical background of sound radiation is given. In Sec. III, we develop the formulation to compute acoustic velocity field from noise sources on a data surface. In Sec. IV, we describe the verification test cases chosen, presenting numerical results. Finally, we end with the conclusions in Sec. V.

II. Radiated Sound Field

We begin with the general form of the FW-H equation [7] as our governing equation given by

$$\left[\frac{1}{c_0^2}\frac{\partial^2}{\partial t^2} - \nabla^2\right]\{p'(\boldsymbol{x},t)\} = q(\boldsymbol{x},t) \tag{1}$$

Received 15 March 2012; revision received 30 June 2012; accepted for publication 31 July 2012; published online 27 November 2012.

*Professor, Pleinlaan 2; ghader.ghorbaniasl@vub.ac.be. Member AIAA.
†Lecturer; m.j.carley@bath.ac.uk.
‡Professor, Pleinlaan 2; chris.lacor@vub.ac.be. Senior Member AIAA.

A key feature of the wave equation obtained for a solid body in a flow is that it is an inhomogeneous wave equation for the external flow problem, embedded in unbounded space. Given the forced wave equation in a stationary medium, the source distribution can be thought of as a distribution of impulsive point sources such that

$$q(\boldsymbol{x},t)=\int_{-\infty}^{t}\int_{-\infty}^{\infty}q(\boldsymbol{y},\tau)\delta(\boldsymbol{x}-\boldsymbol{y})\delta(t-\tau)\,\mathrm{d}^3\boldsymbol{y}\,\mathrm{d}\tau \tag{2}$$

The pulse $\delta(\boldsymbol{x}-\boldsymbol{y})\delta(t-\tau)$ is released at the source point $\boldsymbol{y}$ at time τ, and the fluctuating pressure p' is measured at the observation point $\boldsymbol{x}$ at time t. By using the free space Green's function $G=\delta(g)/r$, where $g=t-\tau-r/c_0$, an integral representation of the solution can be readily found as follows:

$$p'(\boldsymbol{x},t)=\int_{-\infty}^{t}\int_{-\infty}^{\infty}q(\boldsymbol{y},\tau)\frac{\delta(g)}{4\pi r}\,\mathrm{d}^3\boldsymbol{y}\,\mathrm{d}\tau \tag{3}$$

where c_0 stands for the speed of sound, and $r=|\boldsymbol{x}-\boldsymbol{y}|$ is the distance between observer and source. In this equation, the term $q(\boldsymbol{y},\tau)$ consists of three source terms which, because of their physical origin, are called thickness, loading, and quadrupole. In the following, we concentrate on the loading and thickness contributions, which are surface noise sources, dominant in the tone noise of turbomachines. Let

$$q(\boldsymbol{y},\tau)=-\frac{\partial}{\partial x_i}[L_i\delta(f)]+\frac{\partial}{\partial t}[Q\delta(f)] \tag{4}$$

where $\delta(f)$ is the Dirac function for the data surface described by $f(\boldsymbol{y},\tau)=0$. This function has been defined such that $\nabla f=\hat{\boldsymbol{n}}$ [8], which is the outward-pointing unit vector with components of $\hat{n}_i$. The thickness source term Q and the loading source term L_i for a data surface moving with the velocity components v_i are given by

$$Q=\rho(u_n-v_n)+\rho_0 v_n \quad L_i=\rho(u_n-v_n)u_i+p\hat{n}_i \tag{5}$$

where u_i are the fluid velocity vector components. The terms u_n and v_n are, respectively, the fluid and the data surface normal velocity in the frame fixed to the undisturbed medium. The term ρ_0 denotes the density of the undisturbed medium, and p being the local fluid pressure and ρ the local fluid density.

The procedure of the solution for the thickness and loading sources has already been detailed by [9] for the derivation of formulations 1 and 1A in the time domain. Following this procedure gives the loading and the thickness acoustic pressure time history as follows:

$$p'(\boldsymbol{x},t)=p'_T(\boldsymbol{x},t)+p'_L(\boldsymbol{x},t) \tag{6}$$

with

$$\begin{aligned}4\pi p'_T(\boldsymbol{x},t)&=\frac{\partial}{\partial t}\int_S\left[\frac{Q}{r(1-M_r)}\right]_e\mathrm{d}S\\ 4\pi p'_L(\boldsymbol{x},t)&=\frac{1}{c_0}\frac{\partial}{\partial t}\int_S\left[\frac{L_r}{r(1-M_r)}\right]_e\mathrm{d}S+\int_S\left[\frac{L_r}{r^2(1-M_r)}\right]_e\mathrm{d}S\end{aligned} \tag{7}$$

where S represents the moving data surface function defined in a reference frame called the η-frame fixed relative to the data surface. In this equation, $L_r=L_i\hat{r}_i$ and $M_r=M_i\hat{r}_i$, with $\hat{r}_i=|x_i-y_i|/r$ and $M_i=v_i/c_0$. The subscript e indicates that all of the values have to be taken at the retarded time, where $g=0$, i.e., $\tau_e=t-r_e/c_0$ with $r_e=|\boldsymbol{x}-\boldsymbol{y}(\boldsymbol{\eta},\tau_e)|$.

III. Acoustic Velocity Formulations

We can rewrite Eq. (7) in the following form:

$$\begin{aligned}4\pi p'_T(\boldsymbol{x},t)&=\frac{\partial}{\partial t}\int_S\left[\frac{Q}{r(1-M_r)}\right]_e\mathrm{d}S,\\ 4\pi p'_L(\boldsymbol{x},t)&=\frac{\partial}{\partial t}\left\{\frac{1}{c_0}\int_S\left[\frac{L_r}{r(1-M_r)}\right]_e\mathrm{d}S\right.\\ &\quad\left.+\int_0^t\left(\int_S\left[\frac{L_r}{r^2(1-M_r)}\right]_{e^*}\mathrm{d}S\right)\mathrm{d}t^*\right\}\end{aligned} \tag{8}$$

where t^* in the outer integral of the second term on the right denotes the observer time. We have assumed that the body starts to move at $t=0$, so that there is no effect of initial conditions on the acoustic field. The subscript e^* indicates that all of the variables between the bracket have to be calculated at the retarded time τ_{e^*} associated with the observer time t^*, i.e. $\tau_{e^*}=t^*-r_{e^*}/c_0$ where $r_{e^*}=|\boldsymbol{x}-\boldsymbol{y}(\boldsymbol{\eta},\tau_{e^*})|$.

We shall continue with defining a new symbol as follows:

$$p'(\mathrm{x},t)=\frac{\partial B(\boldsymbol{x},t)}{\partial t} \tag{9}$$

Using relations (8) and (9) yields

$$\begin{aligned}4\pi B_T(\boldsymbol{x},t)&=\int_S\left[\frac{Q}{r(1-M_r)}\right]_e\mathrm{d}S\\ 4\pi B_L(\boldsymbol{x},t)&=\frac{1}{c_0}\int_S\left[\frac{L_r}{r(1-M_r)}\right]_e\mathrm{d}S\\ &\quad+\int_0^t\left(\int_S\left[\frac{L_r}{r^2(1-M_r)}\right]_{e^*}\mathrm{d}S\right)\mathrm{d}t^*\end{aligned} \tag{10}$$

where the subscripts T and L denote the thickness part and the loading part of the quantity $B(\boldsymbol{x},t)$, respectively. For the numerical integration in time of the second term on the right-hand side of the expression for loading part, for a small increment Δt, the trapezoidal rule or a rectangular integration in time can be used. Using the rectangular integration role makes the implementation easy without any overhead for computation time. Let $[t_0,t_1,\ldots,t_n]$ be the observer time samples with an increment of Δt. One can approximate the time integration from 0 to an arbitrary observer time $t=t_m$ by

$$I=\sum_{k=0}^{m}\Delta t\int_S\left[\frac{L_r}{r^2(1-M_r)}\right]_{\tau_{e_k}}\mathrm{d}S,\qquad 0\le m<n \tag{11}$$

where τ_{e_k} implies that the retarded time is evaluated at the observer time t_k, i.e. $\tau_{e_k}=\tau_e(\boldsymbol{x},t_k;\boldsymbol{\eta})$. Using relation (11), the loading part of Eq. (10) is approximated by

$$\begin{aligned}4\pi B_L(\boldsymbol{x},t_m)&=\frac{1}{c_0}\int_S\left[\frac{L_r}{r(1-M_r)}\right]_{\tau_{e_m}}\mathrm{d}S\\ &\quad+\sum_{k=0}^{m}\Delta t\int_S\left[\frac{L_r}{r^2(1-M_r)}\right]_{\tau_{e_k}}\mathrm{d}S\end{aligned} \tag{12}$$

It is worth adding that, by taking the Fourier transform of Eq. (9), one obtains the acoustic pressure through the following equation:

$$\tilde{p}'(\boldsymbol{x},f)=i2\pi f\tilde{B}(\boldsymbol{x},f) \tag{13}$$

where the term f represents the frequency of sound and the symbols $\tilde{p}'$ and $\tilde{B}$ denote the Fourier transform of p' and B, respectively. As can be seen, the input data of Eq. (10) come from flow simulations do not need to be differentiated in time or in space. The direct use of the flowfield data can considerably increase the accuracy and speed of noise prediction, in particular, for the broadband noise applications, which deal with the time differentiation of the turbulence data. This is

the subject of another paper by the authors to be submitted for publication.

Now, we turn our attention to the acoustic velocity formulation. We will derive the acoustic velocity potential for an observer fixed to the medium at rest. Assuming that $\phi(\boldsymbol{x}, t)$ is the acoustic velocity potential, we have

$$p'(\boldsymbol{x}, t) = -\rho_0 \frac{\partial \phi(\boldsymbol{x}, t)}{\partial t} \tag{14}$$

Therefore, from Eqs. (9) and (14), one has

$$\phi(\boldsymbol{x}, t) = -\frac{1}{\rho_0} B(\boldsymbol{x}, t) \tag{15}$$

By using relations (10) and (15), the acoustic potential for the thickness and loading sources is given by

$$\begin{aligned} 4\pi\rho_0\phi_T(\boldsymbol{x}, t) &= -\int_S \left[\frac{Q}{r(1-M_r)}\right]_e \mathrm{d}S \\ 4\pi\rho_0\phi_L(\boldsymbol{x}, t) &= -\frac{1}{c_0}\int_S \left[\frac{L_r}{r(1-M_r)}\right]_e \mathrm{d}S \\ &\quad - \int_0^t \left(\int_S \left[\frac{L_r}{r^2(1-M_r)}\right]_{e^*} \mathrm{d}S\right) \mathrm{d}t^* \end{aligned} \tag{16}$$

Let $a_i'(\boldsymbol{x}, t)$ be the acoustic velocity components of the noise generated from the sources. One has

$$a_i'(\boldsymbol{x}, t) = \frac{\partial \phi(\boldsymbol{x}, t)}{\partial x_i} \tag{17}$$

Using Eqs. (16) and (17), the acoustic velocity components for the thickness and loading sources are expressed as follows:

$$\begin{aligned} 4\pi\rho_0 a_{Ti}'(\boldsymbol{x}, t) &= -\int_S \frac{\partial}{\partial x_i}\left[\frac{Q}{r(1-M_r)}\right]_e \mathrm{d}S \\ 4\pi\rho_0 a_{Li}'(\boldsymbol{x}, t) &= -\frac{1}{c_0}\int_S \frac{\partial}{\partial x_i}\left[\frac{L_r}{r(1-M_r)}\right]_e \mathrm{d}S \\ &\quad - \int_0^t \left(\int_S \frac{\partial}{\partial x_i}\left[\frac{L_r}{r^2(1-M_r)}\right]_{e^*} \mathrm{d}S\right) \mathrm{d}t^* \end{aligned} \tag{18}$$

Note that since $\boldsymbol{x}$, $\boldsymbol{\eta}$, and t are independent variables, $\partial/\partial x_i$ was taken inside the integrals (see [9] for more details). To the knowledge of the authors, it is the first time that this formulation is derived.

A. Formulation V1

For time domain formulation of the acoustic velocity components, the gradient operator in Eq. (18) is converted to the time derivative. In general, the terms under the integrals of Eq. (18) are functions of $\boldsymbol{x}$ and t, through $\boldsymbol{y}(\boldsymbol{\eta}, \tau_e)$ and τ_e, as the retarded time τ_e is a function of $\boldsymbol{x}$ and t. Hence, for any function $F(\boldsymbol{x}, \tau_e(\boldsymbol{x}, t))$, one has

$$\left.\frac{\partial F}{\partial x_i}\right|_t = \left.\frac{\partial F}{\partial x_i}\right|_{\tau_e} + \left.\frac{\partial F}{\partial \tau_e}\right|_x \left.\frac{\partial \tau_e}{\partial x_i}\right|_t \tag{19}$$

The first term is a partial derivative describing the explicit x dependence of the function F. With the definition of the retarded time [8], we have

$$\begin{aligned} \left.\frac{\partial \tau_e}{\partial x_i}\right|_t &= -\frac{1}{c_0}\left.\frac{\partial r_e}{\partial x_i}\right|_t = -\frac{1}{c_0}\left[\frac{r_j}{r}\right]_e \left.\frac{\partial (r_j)_e}{\partial x_i}\right|_t \\ &= -\frac{1}{c_0}\left[(\hat{r}_i)_e - (M_r)_e \left.\frac{\partial \tau_e}{\partial x_i}\right|_t\right] \end{aligned} \tag{20}$$

From Eq. (20), one has

$$\left.\frac{\partial \tau_e}{\partial x_i}\right|_t = -\frac{1}{c_0}\left[\frac{\hat{r}_i}{(1-M_r)}\right]_e \tag{21}$$

On the other hand, as already demonstrated by [10], by using the definition of retarded time, one can obtain the following rule:

$$\left.\frac{\partial \tau_e}{\partial t}\right|_x = \left[\frac{1}{(1-M_r)}\right]_e \tag{22}$$

Equation (19) leads to

$$\left.\frac{\partial F}{\partial x_i}\right|_t = \left.\frac{\partial F}{\partial x_i}\right|_{\tau_e} - \frac{(\hat{r}_i)_e}{c_0}\left.\frac{\partial F}{\partial t}\right|_x \tag{23}$$

Applying relation (23) to the thickness term of Eq. (18), removing for the time being the integral, we obtain the following relations:

$$\begin{aligned} \frac{\partial}{\partial x_i}\left(\frac{Q}{r(1-M_r)}\right)_e\Big|_t &= \frac{\partial}{\partial x_i}\left(\frac{Q}{r(1-M_r)}\right)_e\Big|_{\tau_e} \\ &\quad - \frac{(\hat{r}_i)_e}{c_0}\frac{\partial}{\partial t}\left(\frac{Q}{r(1-M_r)}\right)_e\Big|_x \end{aligned} \tag{24}$$

The first term can be evaluated as follows, since the data surface source term does not depend explicitly on $\boldsymbol{x}$:

$$\frac{\partial}{\partial x_i}\left(\frac{Q}{r(1-M_r)}\right)_e\Big|_{\tau_e} = Q(\boldsymbol{y}(\boldsymbol{\eta}, \tau_e))\frac{\partial}{\partial x_i}\left(\frac{1}{r(1-M_r)}\right)_e\Big|_{\tau_e} \tag{25}$$

with

$$\begin{aligned} \frac{\partial}{\partial x_i}\left(\frac{1}{r(1-M_r)}\right)_e\Big|_{\tau_e} &= -\left[\frac{1}{r^2(1-M_r)}\right]_e \left.\frac{\partial r_e}{\partial x_i}\right|_{\tau_e} \\ &\quad + \frac{1}{r_e}\frac{\partial}{\partial x_i}\left(\frac{1}{(1-M_r)}\right)_e\Big|_{\tau_e} \end{aligned} \tag{26}$$

and the relations

$$\begin{aligned} \left.\frac{\partial r_e}{\partial x_i}\right|_{\tau_e} &= (\hat{r}_i)_e, \\ \frac{1}{r_e}\frac{\partial}{\partial x_i}\left(\frac{1}{(1-M_r)}\right)_e\Big|_{\tau_e} &= \frac{1}{r_e}\left[\frac{1}{(1-M_r)^2}\right]_e \left.\frac{\partial (M_r)_e}{\partial x_i}\right|_{\tau_e} \\ &= \frac{1}{r_e}\left[\frac{1}{(1-M_r)^2}\right]_e \left.\frac{\partial (M_j\hat{r}_j)_e}{\partial x_i}\right|_{\tau_e} = \left[\frac{M_j}{r(1-M_r)^2}\right]_e \left.\frac{\partial (\hat{r}_j)_e}{\partial x_i}\right|_{\tau_e} \\ &= \left[\frac{M_j}{r(1-M_r)^2}\right]_e \left[\frac{\delta_{ij} - \hat{r}_i\hat{r}_j}{r}\right]_e = \left[\frac{1}{r^2(1-M_r)^2}\right]_e [M_i - M_e\hat{r}_i]_e \end{aligned} \tag{27}$$

The second term of Eq. (24) is evaluated as follows:

$$\begin{aligned} \frac{(\hat{r}_i)_e}{c_0}\frac{\partial}{\partial t}\left(\frac{Q}{r(1-M_r)}\right)_e\Big|_x &= \frac{1}{c_0}\frac{\partial}{\partial t}\left(\frac{Q\hat{r}_i}{r(1-M_r)}\right)_e\Big|_x \\ &\quad - \frac{1}{c_0}\left[\frac{Q}{r(1-M_r)}\right]_e \left.\frac{\partial (\hat{r}_i)_e}{\partial t}\right|_x \end{aligned} \tag{28}$$

Since

$$\begin{aligned} \left.\frac{\partial (\hat{r}_i)_e}{\partial t}\right|_x &= \left[\frac{1}{r(1-M_r)}\right]_e \left.\frac{\partial (r_i)_e}{\partial \tau_e}\right|_x - \left[\frac{r_i}{r^2(1-M_r)}\right]_e \left.\frac{\partial r_e}{\partial \tau_e}\right|_x \\ &= \left[\frac{-c_0 M_i + c_0\hat{r}_i M_r}{r(1-M_r)}\right]_e \end{aligned} \tag{29}$$

Eq. (28) becomes

$$\frac{(\hat{r}_i)_e}{c_0}\frac{\partial}{\partial t}\left(\frac{Q}{r(1-M_r)}\right)_e\Big|_x = \frac{1}{c_0}\frac{\partial}{\partial t}\left(\frac{Q\hat{r}_i}{r(1-M_r)}\right)_e\Big|_x - \left[\frac{Q}{r^2(1-M_r)^2}\right]_e[-M_i+\hat{r}_iM_r]_e \tag{30}$$

The second term of Eq. (26) is exactly canceled by the second term of Eq. (24). Hence, one obtains

$$\begin{aligned}\frac{\partial}{\partial x_i}\left(\frac{Q}{r(1-M_r)}\right)_e\Big|_t &= Q_e\frac{\partial}{\partial x_i}\left(\frac{1}{r(1-M_r)}\right)_e\Big|_{\tau_e} - \frac{1}{c_0}\frac{\partial}{\partial t}\left(\frac{Q\hat{r}_i}{r(1-M_r)}\right)_e\Big|_x + \frac{1}{c_0}\left[\frac{Q}{r(1-M_r)}\right]_e\frac{\partial(\hat{r}_i)_e}{\partial t}\Big|_x \\ &= -\left[\frac{Qr_i}{r^2(1-M_r)}\right]_e - \frac{1}{c_0}\frac{\partial}{\partial t}\left(\frac{Q\hat{r}_i}{r(1-M_r)}\right)_e\Big|_x \\ &\quad + \left[\frac{Q}{r}\right]_e\left\{\frac{\partial}{\partial x_i}\left(\frac{1}{r(1-M_r)}\right)_e\Big|_{\tau_e} + \left[\frac{1}{c_0(1-M_r)}\right]_e\frac{\partial(\hat{r}_i)_e}{\partial t}\Big|_x\right\}\end{aligned} \tag{31}$$

which reduces to the first two terms

$$\frac{\partial}{\partial x_i}\left(\frac{Q}{r(1-M_r)}\right)_e\Big|_t = -\left[\frac{Q\hat{r}_i}{r^2(1-M_r)}\right]_e - \frac{1}{c_0}\frac{\partial}{\partial t}\left(\frac{Q\hat{r}_i}{r(1-M_r)}\right)_e\Big|_x \tag{32}$$

Based on Eq. (32), the gradient operator of the thickness acoustic velocity component of Eq. (18) can be converted to the time derivative in the following form:

$$4\pi\rho_0 a'_{Ti}(\boldsymbol{x},t) = \frac{1}{c_0}\frac{\partial}{\partial t}\int_S\left[\frac{Q\hat{r}_i}{r(1-M_r)}\right]_e \mathrm{d}S + \int_S\left[\frac{Q\hat{r}_i}{r^2(1-M_r)}\right]_e \mathrm{d}S \tag{33}$$

Since the η frame is time independent, $\partial/\partial t$ of Eq. (33) was taken outside the integral.

To derive the acoustic velocity formulation of the loading noise, one can start with the first term on the right-hand side of Eq. (18) (loading part) as follows:

$$\frac{\partial}{\partial x_i}\left(\frac{L_r}{r(1-M_r)}\right)_e\Big|_t = (\hat{r}_j)_e\frac{\partial}{\partial x_i}\left(\frac{L_j}{r(1-M_r)}\right)_e\Big|_t + \left[\frac{L_j}{r(1-M_r)}\right]_e\frac{\partial(\hat{r}_j)_e}{\partial x_i}\Big|_t \tag{34}$$

Applying Eq. (23) to the gradient operator of the second term on the right-hand side gives

$$\frac{\partial(\hat{r}_j)_e}{\partial x_i}\Big|_t = \frac{\partial(\hat{r}_j)_e}{\partial x_i}\Big|_{\tau_e} - \frac{(\hat{r}_i)_e}{c_0}\frac{\partial(\hat{r}_j)_e}{\partial t}\Big|_x \tag{35}$$

Since

$$\frac{\partial(\hat{r}_j)_e}{\partial x_i}\Big|_{\tau_e} = \frac{\partial}{\partial x_i}\left(\frac{r_j}{r}\right)_e\Big|_{\tau_e}\left[\frac{\delta_{ij}-\hat{r}_i\hat{r}_j}{r}\right]_e \tag{36}$$

one has

$$\frac{\partial(\hat{r}_j)_e}{\partial x_i}\Big|_t = \left[\frac{\delta_{ij}-\hat{r}_i\hat{r}_j}{r}\right]_e - \frac{(\hat{r}_i)_e}{c_0}\frac{\partial(\hat{r}_j)_e}{\partial t}\Big|_x \tag{37}$$

Therefore, Eq. (34) yields

$$\frac{\partial}{\partial x_i}\left(\frac{L_r}{r(1-M_r)}\right)_e\Big|_t = (\hat{r}_j)_e\frac{\partial}{\partial x_i}\left(\frac{L_j}{r(1-M_r)}\right)_e\Big|_t + \left[\frac{L_i-\hat{r}_iL_r}{r^2(1-M_r)}\right]_e - \frac{1}{c_0}\left[\frac{L_j\hat{r}_i}{r(1-M_r)}\right]_e\frac{\partial(\hat{r}_j)_e}{\partial t}\Big|_x \tag{38}$$

According to relation (23), the first term on the right-hand side of Eq. (38) is given by

$$\begin{aligned}(\hat{r}_j)_e\frac{\partial}{\partial x_i}\left(\frac{L_j}{r(1-M_r)}\right)_e\Big|_t &= -\frac{(\hat{r}_j)_e}{c_0}\frac{\partial}{\partial t}\left(\frac{L_j\hat{r}_i}{r(1-M_r)}\right)_e\Big|_x - \left[\frac{L_r\hat{r}_i}{r^2(1-M_r)}\right]_e \\ &= -\frac{1}{c_0}\frac{\partial}{\partial t}\left(\frac{L_r\hat{r}_i}{r(1-M_r)}\right)_e\Big|_x + \frac{1}{c_0}\left[\frac{L_j\hat{r}_i}{r(1-M_r)}\right]_e\frac{\partial(\hat{r}_j)_e}{\partial t}\Big|_x - \left[\frac{L_r\hat{r}_i}{r^2(1-M_r)}\right]_e\end{aligned} \tag{39}$$

Substituting Eq. (39) into Eq. (38) will give

$$\frac{\partial}{\partial x_i}\left(\frac{L_r}{r(1-M_r)}\right)_e\Big|_t = -\frac{1}{c_0}\frac{\partial}{\partial t}\left(\frac{L_r\hat{r}_i}{r(1-M_r)}\right)_e\Big|_x + \left[\frac{L_i-2L_r\hat{r}_i}{r^2(1-M_r)}\right]_e \tag{40}$$

Similarly, one can obtain the following relation for the second term on the right-hand side of the loading part of Eq. (18). Let

$$\frac{\partial}{\partial x_i}\left(\frac{L_r}{r^2(1-M_r)}\right)_{e^*}\Big|_t = \frac{1}{r_{e^*}}\frac{\partial}{\partial x_i}\left(\frac{L_r}{r(1-M_r)}\right)_{e^*}\Big|_t - \left[\frac{L_r}{r^3(1-M_r)}\right]_{e^*}\frac{\partial r_{e^*}}{\partial x_i}\Big|_t \tag{41}$$

From relation (23),

$$\frac{\partial r_{e^*}}{\partial x_i}\Big|_t = \frac{\partial r_{e^*}}{\partial x_i}\Big|_{\tau_{e^*}} - \frac{(\hat{r}_i)_{e^*}}{c_0}\frac{\partial r_{e^*}}{\partial t}\Big|_x = (\hat{r}_i)_{e^*} - \frac{(\hat{r}_i)_{e^*}}{c_0}\frac{\partial r_{e^*}}{\partial t}\Big|_x \tag{42}$$

Eq. (41) becomes

$$\frac{\partial}{\partial x_i}\left(\frac{L_r}{r^2(1-M_r)}\right)_{e^*}\Big|_t = \frac{1}{r_{e^*}}\frac{\partial}{\partial x_i}\left(\frac{L_r}{r(1-M_r)}\right)_{e^*}\Big|_t - \left[\frac{L_r\hat{r}_i}{r^3(1-M_r)}\right]_{e^*} + \frac{1}{c_0}\left(\frac{L_r\hat{r}_i}{r^3(1-M_r)}\right)_{e^*}\frac{\partial r_{e^*}}{\partial t}\Big|_x \tag{43}$$

using relation (40)

$$\begin{aligned}\frac{1}{r_{e^*}}\frac{\partial}{\partial x_i}\left(\frac{L_r}{r(1-M_r)}\right)_{e^*}\Big|_t &= -\frac{1}{r_{e^*}}\frac{1}{c_0}\frac{\partial}{\partial t}\left(\frac{L_r\hat{r}_i}{r(1-M_r)}\right)_{e^*}\Big|_x + \left[\frac{L_i-2L_r\hat{r}_i}{r^3(1-M_r)}\right]_{e^*} \\ &= -\frac{1}{c_0}\frac{\partial}{\partial t}\left(\frac{L_r\hat{r}_i}{r^2(1-M_r)}\right)_{e^*}\Big|_x - \frac{1}{c_0}\left[\frac{L_r\hat{r}_i}{r^3(1-M_r)}\right]_{e^*}\frac{\partial(r_i)_{e^*}}{\partial t}\Big|_x + \left[\frac{L_i-2L_r\hat{r}_i}{r^3(1-M_r)}\right]_{e^*}\end{aligned} \tag{44}$$

Substituting Eq. (44) into Eq. (43) gives

$$\frac{\partial}{\partial x_i}\left(\frac{L_r}{r^2(1-M_r)}\right)_{e^*}\Big|_t = -\frac{1}{c_0}\frac{\partial}{\partial t}\left(\frac{L_r\hat{r}_i}{r^2(1-M_r)}\right)_{e^*}\Big|_x + \left[\frac{L_i-3L_r\hat{r}_i}{r^3(1-M_r)}\right]_{e^*} \tag{45}$$

Substituting relations (40) and (45) into the loading part of Eq. (18) yields

$$4\pi\rho_0 a'_{Li}(\boldsymbol{x},t) = \frac{1}{c_0^2}\frac{\partial}{\partial t}\int_S \left[\frac{\hat{r}_i L_r}{r(1-M_r)}\right]_e \mathrm{d}S - \frac{1}{c_0}\int_S \left[\frac{L_i - 2\hat{r}_i L_r}{r^2(1-M_r)}\right]_e \mathrm{d}S - \frac{1}{c_0}\int_S \left[\frac{\hat{r}_i L_r}{r^2(1-M_r)}\right]_e \mathrm{d}S - \int_0^t \left(\int_S \left[\frac{L_i - 3\hat{r}_i L_r}{r^3(1-M_r)}\right]_{e^*} \mathrm{d}S\right) \mathrm{d}t^* \tag{46}$$

This equation reduces to

$$4\pi\rho_0 a'_{Li}(\boldsymbol{x},t) = \frac{1}{c_0^2}\frac{\partial}{\partial t}\int_S \left[\frac{\hat{r}_i L_r}{r(1-M_r)}\right]_e \mathrm{d}S - \frac{1}{c_0}\int_S \left[\frac{L_i - 3\hat{r}_i L_r}{r^2(1-M_r)}\right]_e \mathrm{d}S - \int_0^t \left(\int_S \left[\frac{L_i - 3\hat{r}_i L_r}{r^3(1-M_r)}\right]_{e^*} \mathrm{d}S\right) \mathrm{d}t^* \tag{47}$$

Equations (33) and (47) are called formulation V1 (V denotes velocity) of Ghorbaniasl, being the analogous to formulation 1 [9] for the acoustic pressure fluctuations. In this formulation, the observer time derivatives are also outside of the integral.

B. Formulation V1A

Eliminating the numerical differentiation improves the speed and accuracy of the calculation [11]. For this reason, the time derivative of formulation 1 was taken inside the integrals and formulation 1A [9] was derived. Based on the same philosophy, the time derivatives of formulation V1 are taken inside the integrals as in the following equations.

1. *Thickness Sources*

Starting from Eq. (33) and considering that the data surface frame is time independent, one takes the time derivative inside the integral and obtains

$$\frac{\partial}{\partial t}\int_S \left[\frac{Q\hat{r}_i}{r(1-M_r)}\right]_e \mathrm{d}S = \int_S \left[\hat{r}_i \frac{\partial}{\partial t}\left(\frac{Q}{r(1-M_r)}\right)\right]_e \mathrm{d}S + \int_S \left[\frac{Q}{r(1-M_r)}\frac{\partial \hat{r}_i}{\partial t}\right]_e \mathrm{d}S \tag{48}$$

Applying relation (29) to the second term of the right-hand side of Eq. (48) gives

$$\int_S \left[\frac{Q}{r(1-M_r)}\frac{\partial \hat{r}_i}{\partial t}\right]_e \mathrm{d}S = c_0 \int_S \left[Q\frac{M_r\hat{r}_i - M_i}{r^2(1-M_r)^2}\right]_e \mathrm{d}S \tag{49}$$

Therefore, Eq. (33) becomes

$$4\pi\rho_0 a'_{Ti}(\boldsymbol{x},t) = \frac{1}{c_0}\int_S \left[\hat{r}_i \frac{\partial}{\partial t}\left(\frac{Q}{r(1-M_r)}\right)\right]_e \mathrm{d}S + \int_S \left[Q\frac{M_r\hat{r}_i - M_i}{r^2(1-M_r)^2}\right]_e \mathrm{d}S + \int_S \left[\frac{Q\hat{r}_i}{r^2(1-M_r)}\right]_e \mathrm{d}S \tag{50}$$

or

$$4\pi\rho_0 a'_{Ti}(\boldsymbol{x},t) = \frac{1}{c_0}\int_S \left[\hat{r}_i \frac{\partial}{\partial t}\left(\frac{Q}{r(1-M_r)}\right)\right]_e \mathrm{d}S - \int_S \left[Q\frac{M_i - \hat{r}_i}{r^2(1-M_r)^2}\right]_e \mathrm{d}S \tag{51}$$

The thickness noise integrand of the formulation 1 can be observed in the first term on the right-hand side of this equation. Let

$$I_T = \frac{\partial}{\partial t}\left[\frac{Q}{r(1-M_r)}\right] = \frac{1}{1-M_r}\frac{\partial}{\partial \tau}\left[\frac{Q}{r(1-M_r)}\right] \tag{52}$$

Expansion of this expression in the same manner as in the derivation of formulation 1A gives

$$I_T = \frac{\dot{Q}}{r(1-M_r)^2} + Q\frac{r\dot{M}_r + c_0(M_r - M^2)}{r^2(1-M_r)^3} \tag{53}$$

where $\dot{M}_r = \dot{M}_i\hat{r}_i$. The dot over the quantity implies the differentiation of this magnitude with respect to the emission time.

Finally, the acoustic velocity components for the thickness sources are obtained as follows:

$$4\pi\rho_0 a'_{Ti}(\boldsymbol{x},t) = \frac{1}{c_0}\int_S [\hat{r}_i I_T]_e \,\mathrm{d}S - \int_S \left[Q\frac{M_i - \hat{r}_i}{r^2(1-M_r)^2}\right]_e \mathrm{d}S \tag{54}$$

2. *Loading Sources*

One can rewrite Eq. (47) as follows:

$$4\pi\rho_0 a'_{Li}(\boldsymbol{x},t) = \frac{1}{c_0^2}\int_S \hat{r}_i \frac{\partial}{\partial t}\left[\frac{L_r}{r(1-M_r)}\right]_e \mathrm{d}S + \frac{1}{c_0^2}\int_S \left[\frac{L_r}{r(1-M_r)}\frac{\partial \hat{r}_i}{\partial t}\right]_e \mathrm{d}S - \frac{1}{c_0}\int_S \left[\frac{L_i - 3\hat{r}_i L_r}{r^2(1-M_r)}\right]_e \mathrm{d}S - \int_0^t \left(\int_S \left[\frac{L_i - 3\hat{r}_i L_r}{r^3(1-M_r)}\right]_{e^*} \mathrm{d}S\right) \mathrm{d}t^* \tag{55}$$

Using relation (29) and rearranging the terms, we have

$$4\pi\rho_0 a'_{Li}(\boldsymbol{x},t) = \frac{1}{c_0}\int_S \left[\hat{r}_i\left(\frac{1}{c_0}\frac{\partial}{\partial t}\left[\frac{L_r}{r(1-M_r)}\right]_e + \left[\frac{L_r}{r^2(1-M_r)}\right]\right)\right]_e \mathrm{d}S - \frac{1}{c_0}\int_S \left[L_r\frac{M_i - \hat{r}_i}{r^2(1-M_r)^2}\right]_e \mathrm{d}S - \frac{1}{c_0}\int_S \left[\frac{L_i - L_r\hat{r}_i}{r^2(1-M_r)}\right]_e \mathrm{d}S - \int_0^t \left(\int_S \left[\frac{L_i - 3L_r\hat{r}_i}{r^3(1-M_r)}\right]_{e^*} \mathrm{d}S\right) \mathrm{d}t^* \tag{56}$$

It is observed that the loading noise integrand of formulation 1 denoted by I_L appears in the first term on the right-hand side of Eq. (56). Let

$$I_L = \frac{1}{c_0}\frac{\partial}{\partial t}\left[\frac{L_r}{r(1-M_r)}\right]_e + \left[\frac{L_r}{r^2(1-M_r)}\right] \tag{57}$$

Expansion of this expression in the same manner as in the derivation of formulation 1A gives

$$I_L = \frac{1}{c_0}\frac{\dot{L}_r}{r(1-M_r)^2} + \frac{L_r - L_M}{r^2(1-M_r)^2} + \frac{1}{c_0}L_r\frac{r\dot{M}_r + c_0(M_r - M^2)}{r^2(1-M_r)^3} \tag{58}$$

with

$$\dot{L}_r = \dot{L}_i\hat{r}_i, \qquad L_M = L_i M_i \tag{59}$$

Finally, the acoustic velocity components for the loading sources are given by

$$4\pi\rho_0 a'_{Li}(\boldsymbol{x},t) = \frac{1}{c_0}\int_S [\hat{r}_i I_L]_e \,\mathrm{d}S - \frac{1}{c_0}\int_S \left[L_r\frac{M_i - \hat{r}_i}{r^2(1-M_r)^2}\right]_e \mathrm{d}S - \frac{1}{c_0}\int_S \left[\frac{L_i - L_r\hat{r}_i}{r^2(1-M_r)}\right]_e \mathrm{d}S - \int_0^t \left(\int_S \left[\frac{L_i - 3L_r\hat{r}_i}{r^3(1-M_r)}\right]_{e^*} \mathrm{d}S\right) \mathrm{d}t^* \tag{60}$$

Equations (54) and (60) together with relations (53) and (58) are referred to as formulation V1A of Ghorbaniasl, being analogous to the formulation 1A for the acoustic pressure fluctuations. This

formulation is numerically more efficient since the numerical time derivative of formulation V1 has been eliminated. This formulation is valid for bodies with a complex geometry and an arbitrary motion. Note that formulations V1 and V1A are derived for an observer fixed to undisturbed medium.

The time integration in the loading part adds very little overhead to the computation, since it is computed using a trapezoidal rule on the time series for velocity, adding only a small amount of extra work at each time point, as the new point is added to the trapezoidal rule. However, we propose to use a rectangular integration rule in which there is not any extra work due to this integration on the time series for velocity. We have shown the procedure in Fig. 1. A compact form of Eq. (60) is used in this diagram,

$$4\pi\rho_0 a'_{Li}(\boldsymbol{x},t) = I_1 - \int_0^t I_2 \,\mathrm{d}t^*$$

For each observer time point, the acoustic velocity is evaluated by summing I_1 and I_2 in the same fashion as done in formulation 1A. It can be observed that the time integration part is performed at the same time as the acoustic velocity is computed for each observer time, and there is no overhead when this rectangular time integration rule is used. It will be shown with numerical examples that formulation V1A requires the same amount of computation time as formulation 1A.

The advantage of formulation V1A over formulation G1A is that, first, it is mathematically much more compact than formulation G1A. This property makes the formulation easy to implement. Second, it obviates the need of computing second-order time derivatives at each observer time, which makes formulation G1A computationally expensive. As demonstrated by [6], formulation G1A requires three times as much computation time as formulation 1A. The reduction of computation time can be very important for the formulation when it is applied for noise scattering problems. Variables with the second-order time derivatives inside integrals can also reduce the accuracy of simulations. We should also mention that because formulation V1A computes the acoustic velocity directly, there is no need for the extra computations required by formulation G1A for acoustic velocity determination.

It is worth adding that formulation V1A is much similar to formulation G1 in the form, except that the time derivative of formulation G1 outside the integrals must still be performed. The speed and accuracy of the noise calculation is improved by the elimination of the time derivative. The accuracy of the simulation is also very sensitive to the algorithm chosen for handling the time derivative outside the integrals. In order to overcome this problem the time derivative outside the integrals is eliminated and formulation G1A is developed. Based on the same reason, formulation 1A has been obtained from formulation 1. As [6] showed, formulation G1 requires approximately five times as much computation time as formulation 1A. Taking the time derivative inside the integrals of G1 increases the speed and the accuracy but leads to a long formula of G1A. It involves terms with second time derivatives inside integrals, which can disturb accuracy and decrease the speed. Formulation V1A only contains the variable of formulation 1A, which is a very important from numerical point of view.

The simple case of a stationary data surface is commonly used in the hybrid CFD/acoustic analogy approach. In this case, $M = 0$ and formulation V1A reduces to

$$4\pi\rho_0 a'_{Ti}(\boldsymbol{x},t) = \frac{1}{c_0}\int_S [\hat{r}_i I_T]_e \,\mathrm{d}S - \int_S \left[Q\frac{-\hat{r}_i}{r^2}\right]_e \mathrm{d}S$$

$$4\pi\rho_0 a'_{Li}(\boldsymbol{x},t) = \frac{1}{c_0}\int_S [\hat{r}_i I_L]_e \,\mathrm{d}S - \frac{1}{c_0}\int_S \left[L_r\frac{-\hat{r}_i}{r^2}\right]_e \mathrm{d}S - \frac{1}{c_0}\int_S \left[\frac{L_i - \hat{r}_i L_r}{r^2}\right]_e \mathrm{d}S - \int_0^t \left(\int_S \left[\frac{L_i - 3\hat{r}_i L_r}{r^3}\right]_{e^*} \mathrm{d}S\right)\mathrm{d}t^* \quad (61)$$

where

$$I_T = \frac{\dot{Q}}{r} \qquad I_L = \frac{1}{c_0}\frac{\dot{L}_r}{r} + \frac{L_r}{r^2} \quad (62)$$

In this case, the emission distance between the observer and the source is constant, and the radius r does not depend on the retarded time. Therefore, the retarded time is obtained with an explicit solution, where no iterative method is needed. This reduces the computational time.

IV. Numerical Results

In this section, the acoustic velocity field simulated by the derived formulation is validated through three test cases. The first case considers a 3-D monopole source, which is identified with a pulsating sphere. The second test case contains a 3-D dipole source. The third test case is the consistency test known as the Isom thickness noise [12]. Showing the quality and reliability of the developed formulation for acoustic scattering problems and real flows is our future work.

A. Test Case 1: Pulsating Sphere

In order to verify the numerical algorithms, the analytical solution of a 3-D monopole source has been used. A 3-D monopole is identified with a pulsating sphere as the small sphere with a radius a in Fig. 2. The pressure fluctuation induced by the pulsating sphere is represented by a harmonic spherical wave

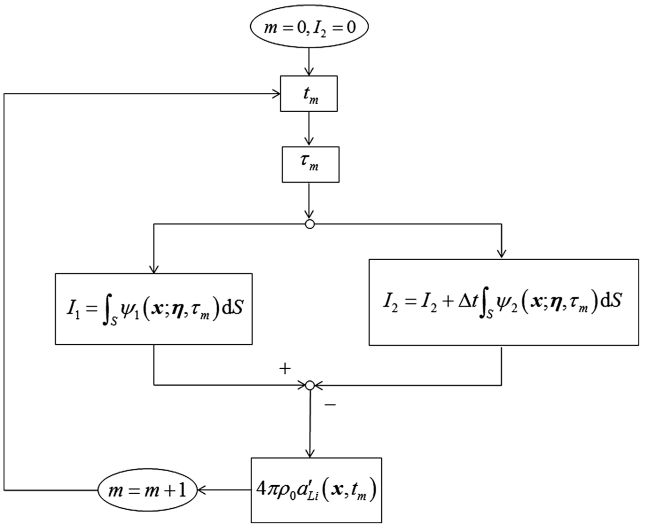

Fig. 1 The procedure for the time history loading part of acoustic velocity is shown.

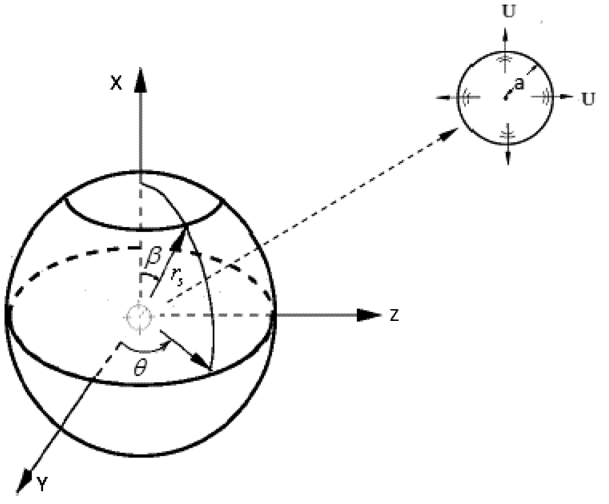

Fig. 2 Monopole source and data surface are shown.

$$p'(r,t) = \frac{A\omega\rho_0}{4\pi r}\frac{1}{\sqrt{1+(ka)^2}}\cos[\omega t - k(r-a) + \phi_0] \quad (63)$$

where ω and k are, respectively, the angular velocity and the wave number of the fluctuations, and

$$\phi_0 = \tan^{-1}(1/ka) \quad r = \sqrt{x^2+y^2+z^2} \quad (64)$$

The velocity is easily obtained with

$$u_r(r,t) = \frac{1}{\sqrt{1+(ka)^2}}\left\{\frac{Ak}{4\pi r}\cos[\omega t - k(r-a) + \phi_0] + \frac{A}{4\pi r^2}\sin[\omega t - k(r-a) + \phi_0]\right\} \quad (65)$$

In the preceding equations, the term A equals $4\pi a^2 U$ (see Fig. 2). One can also obtain the velocity components in the Cartesian frame as

$$u = \frac{x}{r}u_r \quad v = \frac{y}{r}u_r \quad w = \frac{z}{r}u_r \quad (66)$$

To perform the calculation for this test case, we take the radius of the spherical penetrable data surface r_s to be $3.25a$. The large sphere with radius r_s in Fig. 2 is the data surface, which contains the sources obtained from Eqs. (63) and (66). The ambient speed of sound c_0 is set to be 340 m/s. The density for the undisturbed medium is assumed to be 1.2 kg/m^3. The angular frequency ω of the source is 1020 rad/s. The other parameters are $a = 0.01$ m and $U = 8$ m/s. The total number of computational grid points is 4095. The grid points are well distributed on the spherical surface with increments of $\Delta\theta$ and $\Delta\beta$ equal to 4 deg. This resolution for the data surface with a radius of $r_s = 0.0325$ m was fine enough. The temporal resolution is fine enough, namely, $\Delta t/T$ is smaller than 0.02. The observer distance is assumed to be $R = 20$ m.

The numerical method is applied to this test case, and the acoustic velocity components are calculated. The calculated results are compared with analytical solutions for different observer positions. The x, y, and z components of the acoustic velocity obtained with formulation V1A is plotted in Figs. 3–5, respectively. As can be seen, there is a very good agreement between the numerical method and the analytical solution. This excellent agreement between the results verifies that the formulation predicts the acoustic velocity components accurately for this case.

B. Test Case 2: A Three-Dimensional Dipole Source

A compact oscillating sphere, which is equivalent to two very closely positioned monopole point sources with opposite fluctuation phases, is denoted as a dipole point source. A dipole has an axis, which is the line connecting the centers of the two nearby monopoles (pulsating spheres with radius of a). The monopoles are positioned in the y direction with a distance of $d/2 = 1.25a$ from the center (d is the distance between the two monopole points). The pressure fluctuation induced by the two monopoles for an observer positioned at (x, y, z) is

$$p'(r,t) = -\frac{A\omega\rho_0}{4\pi r_1}\frac{1}{\sqrt{1+(ka)^2}}\cos[\omega t - k(r_1-a) + \phi_0] + \frac{A\omega\rho_0}{4\pi r_2}\frac{1}{\sqrt{1+(ka)^2}}\cos[\omega t - k(r_2-a) + \phi_0] \quad (67)$$

with

$$\phi_0 = \tan^{-1}(1/ka) \quad r_1 = \sqrt{x^2+(y+0.5d)^2+z^2} \quad r_2 = \sqrt{x^2+(y-0.5d)^2+z^2} \quad (68)$$

The problem parameters are the same as those of the previous problem. For this source, the particle velocity components in Cartesian coordinates are

$$u = -\frac{x}{r_1}u_r(r_1,t) + \frac{x}{r_2}u_r(r_2,t)$$
$$v = -\frac{y+0.5d}{r_1}u_r(r_1,t) + \frac{y-0.5d}{r_2}u_r(r_2,t)$$
$$w = -\frac{z}{r_1}u_r(r_1,t) + \frac{z}{r_2}u_r(r_2,t) \quad (69)$$

where the terms $u_r(r,t)$ are obtained from Eq. (65).

The integration surface used in the previous test case is also used here, i.e., $r_s = 3.25a$ m. The following parameters are used: $\omega = 1020$ rad/s, $a = 0.01$ m, $U = 8$ m/s, $c_0 = 340$ m/s, and $\rho_0 = 1.2$ kg/m^3. The flow parameters and the observer distance are chosen the same as in the previous case.

There are 7200 panels on the spherical penetrable surface. In order to record the acoustic time history, 256 observer time points are used per period. The computation is performed for this test case, and the acoustic velocity components are calculated. The computed results are compared with those of the analytical solution, showing for different observer positions. As shown in Figs. 6–8, the numerical and analytical methods match each other quite well.

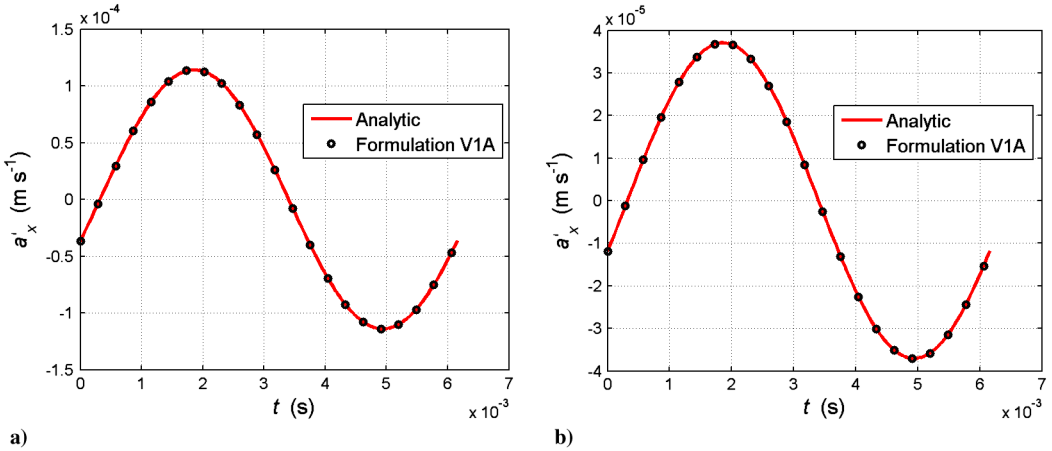

Fig. 3 The calculated x-component of acoustic velocity compared with that of the analytical solution is shown for different observer positions. a) $\beta = 18$ deg; b) $\beta = 72$ deg. Monopole source point.

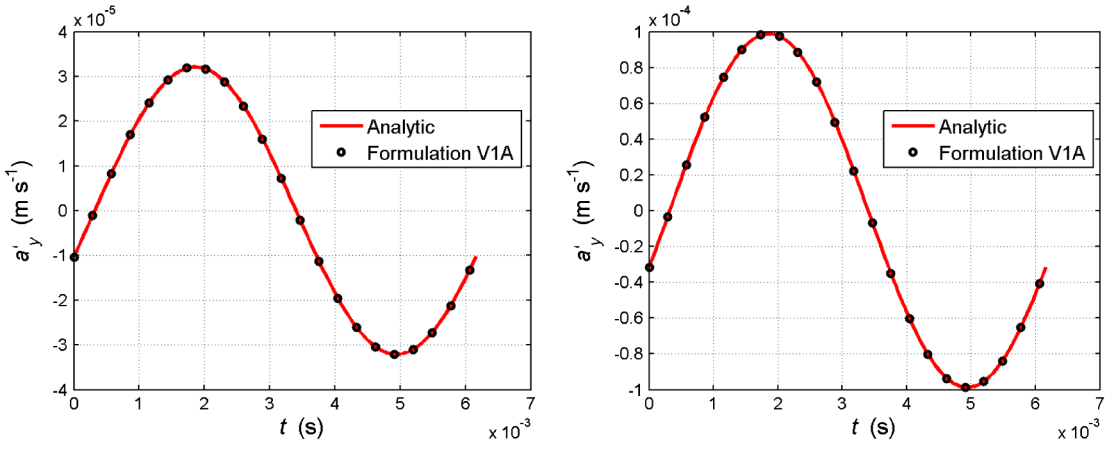

a) b)

Fig. 4 The calculated *y*-component of acoustic velocity compared with that of the analytical solution is shown for different observer positions. a) $\beta = 18$ deg; b) $\beta = 72$ deg. Monopole source point.

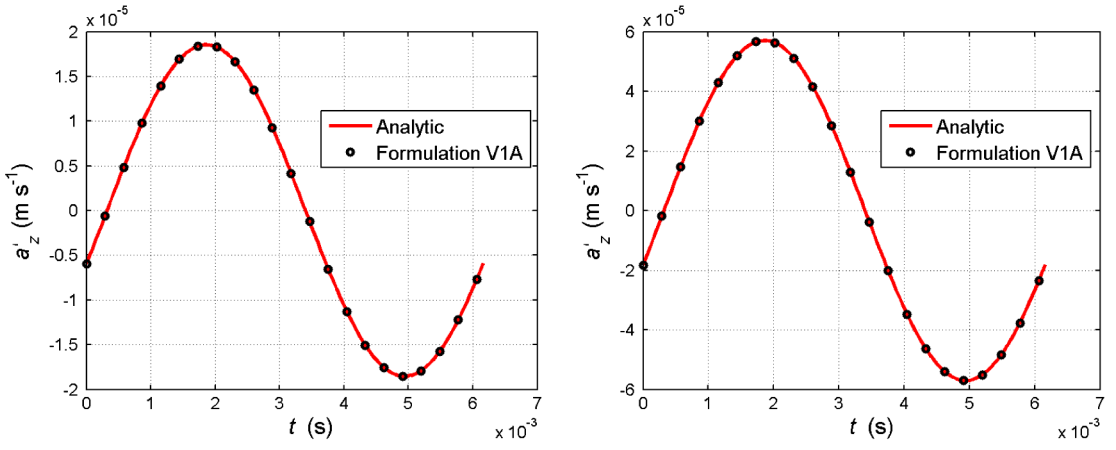

a) b)

Fig. 5 The calculated *z*-component of acoustic velocity compared with that of the analytical solution is shown for different observer positions. a) $\beta = 18$ deg; b) $\beta = 72$ deg. Monopole source point.

C. Test Case 3: Isom Noise Consistency

The Isom thickness noise property [12–14] is described in [15]. It is demonstrated that if a constant aerodynamic load, $p = \rho_0 c_0^2$ is applied over a moving surface the generated dipole noise should be identical to the monopole thickness noise contribution.

This consistency has already been tested for a conventional helicopter blade [16]. It was shown that by including the blade tip source and refining the grid at the inner and outer radii of the blade, the calculated Isom noise results match the monopole noise results quite well. It was also indicated that by decreasing the thickness ratio

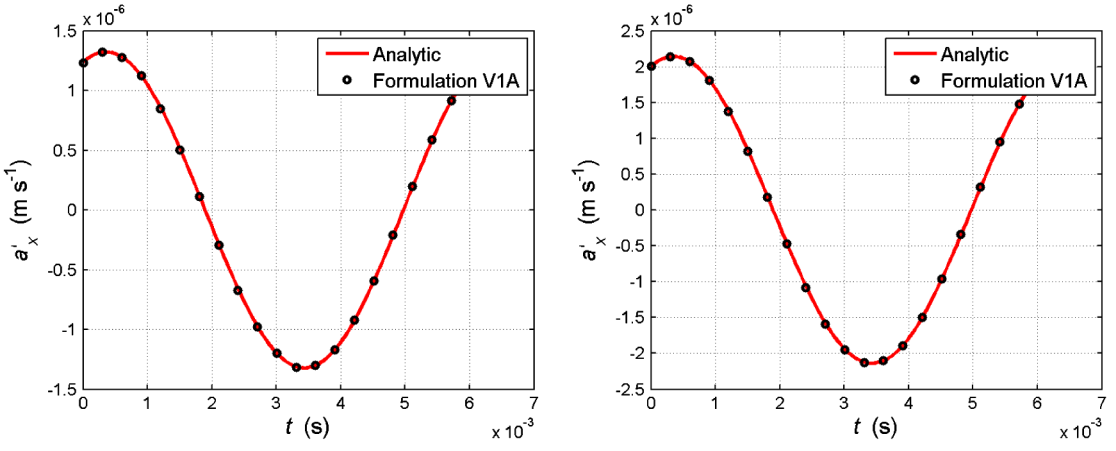

a) b)

Fig. 6 The calculated *x*-component of acoustic velocity compared with that of the analytical solution is shown for different observer positions. a) $\beta = 18$ deg; b) $\beta = 36$ deg. Dipole source point.

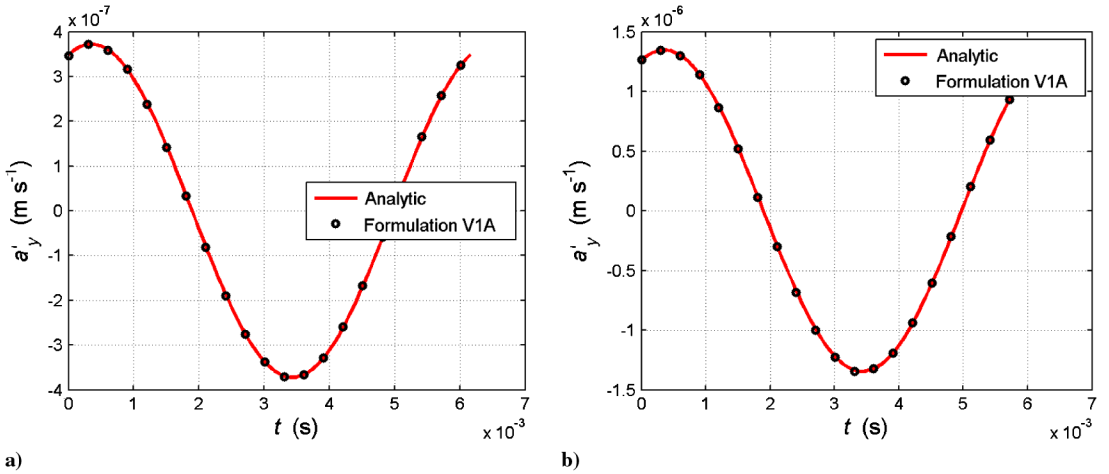

a) b)

Fig. 7 The calculated y-component of acoustic velocity compared with that of the analytical solution is shown for different observer positions. a) $\beta = 18$ deg; b) $\beta = 36$ deg. Dipole source point.

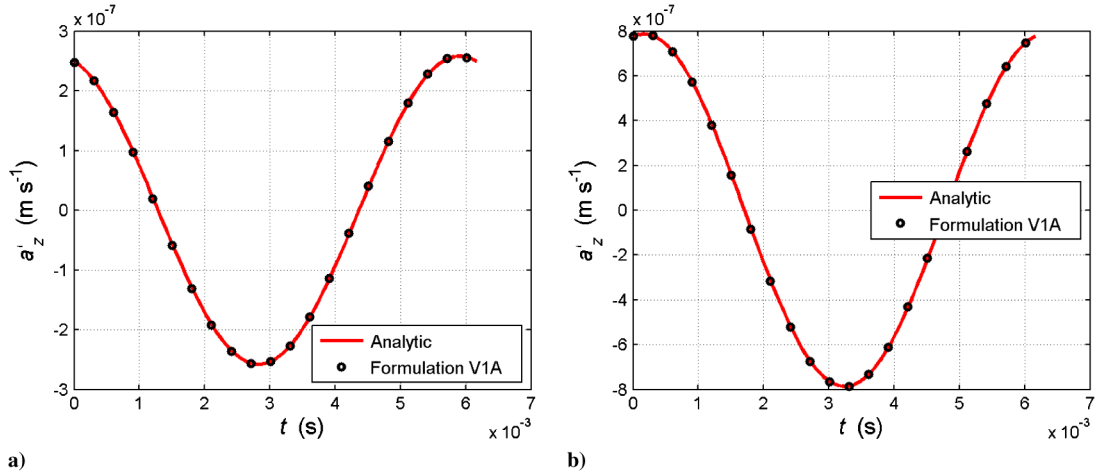

a) b)

Fig. 8 The calculated z-component of acoustic velocity compared with that of the analytical solution is shown for different observer positions. a) $\beta = 18$ deg; b) $\beta = 36$ deg. Dipole source point.

at the extremities of the blade the calculated results agree with the theory. The sensitivity of the Isom noise consistency test to temporal resolution, Mach number, source-observer distance, and interpolation algorithm type has been studied in [17].

In the present work, we will show that the Isom noise consistency test is also valid for the acoustic velocity field. According to the relation between the acoustic pressure and the acoustic velocity potential or the relation of $\partial p'/\partial x_i = -\rho_0 \partial a'_i/\partial t$, this is theoretically valid. We will show a numerical confirmation of this consistency for the acoustic velocity. Furthermore, it will be shown that if dipole noise is induced by a uniform distribution of the load $p = \rho_0 c_0^2$ on the entire moving data surface the generated acoustic velocity components are identical to those generated by the thickness source.

The numerical strategy is applied to the noise generated by the flow around a conventional helicopter rotor test case. The helicopter rotor consists of two equally spaced blades 10 m in diameter with a constant chord of 0.4 m. The thickness ratio of the blades is 10%, which vanishes at the inner and outer radii of the blade. The schematic of the blade geometry and its thickness ratio decreasing at the extremities are shown in Fig. 9. The blade tip Mach number is fixed at 0.8. The observer is located 50 m from the origin of the blade-fixed frame.

The blade surface is discretized into 75 cells around the blade airfoil and 100 divisions along the radial direction for complete convergence. A nonuniform mesh density is used in both directions. A calculation is performed for 128 time points per blade passage to resolve the pressure time history.

The x, y, and z components of the acoustic velocity generated by the Isom source are shown in Figs. 10–12, respectively. The associated acoustic velocity components generated by the thickness noise source are also plotted in these figures for comparison. As can be seen, there is excellent agreement between the acoustic velocity due to the Isom thickness noise source and that from the thickness noise source. The agreement between the results is observed for different acoustic velocity components and for all of the observer positions chosen. This agreement confirms that the derived formulation can be used to accurately compute the acoustic velocity for the monopole and dipole type sources on the data surface.

Formulation 1A is considered as a reference and the computational time for formulation V1A is evaluated for test cases used. Table 1

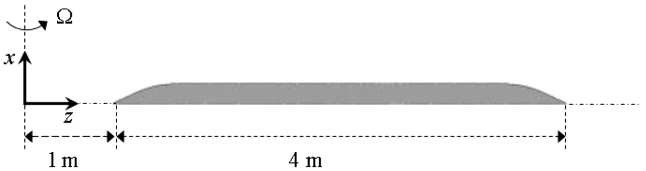

Fig. 9 Blade geometry and its decreased thickness ratio at the extremities are shown.

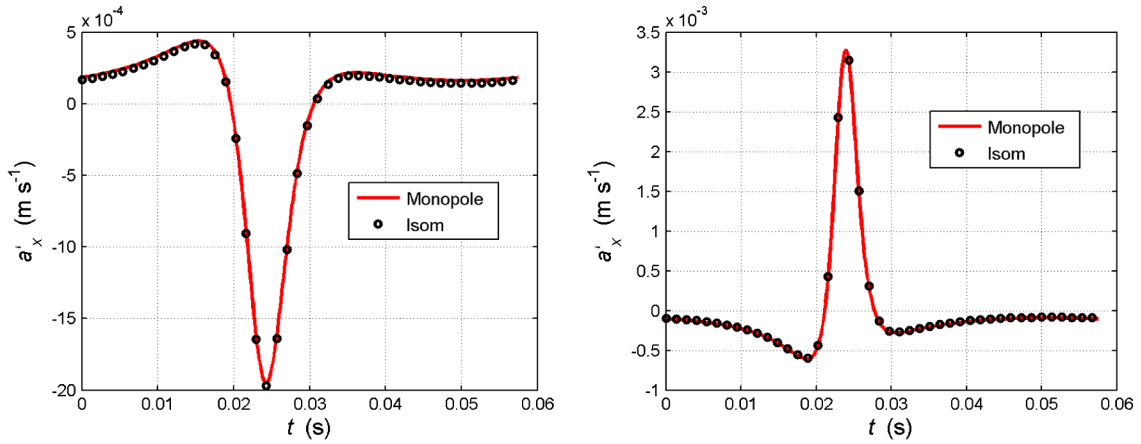

a) b)

Fig. 10 The calculated x-component of acoustic velocity generated by Isom noise source is compared with that of the thickness noise source for different observer positions. a) $\beta = 54$ deg; b) $\beta = 108$ deg.

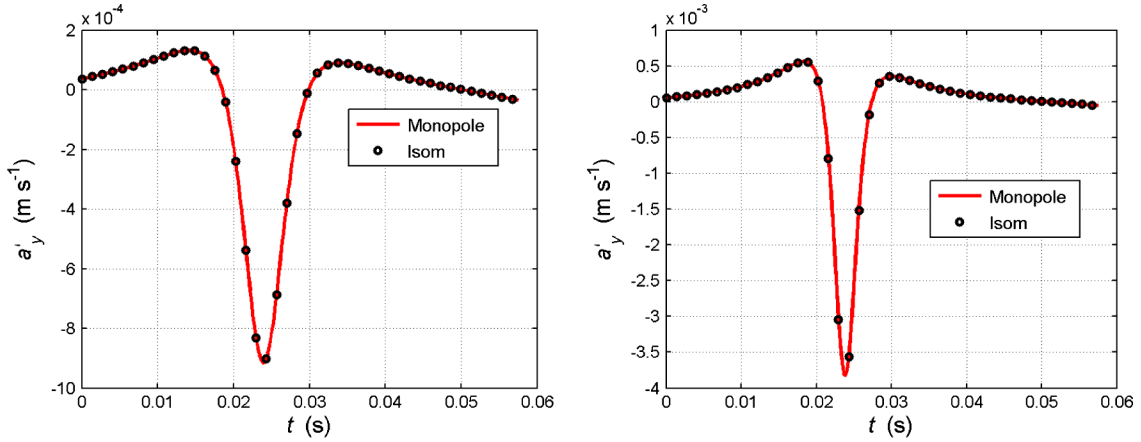

a) b)

Fig. 11 The calculated y-component of acoustic velocity generated by Isom noise source is compared with that of the thickness noise source for different observer positions. a) $\beta = 54$ deg; b) $\beta = 108$ deg.

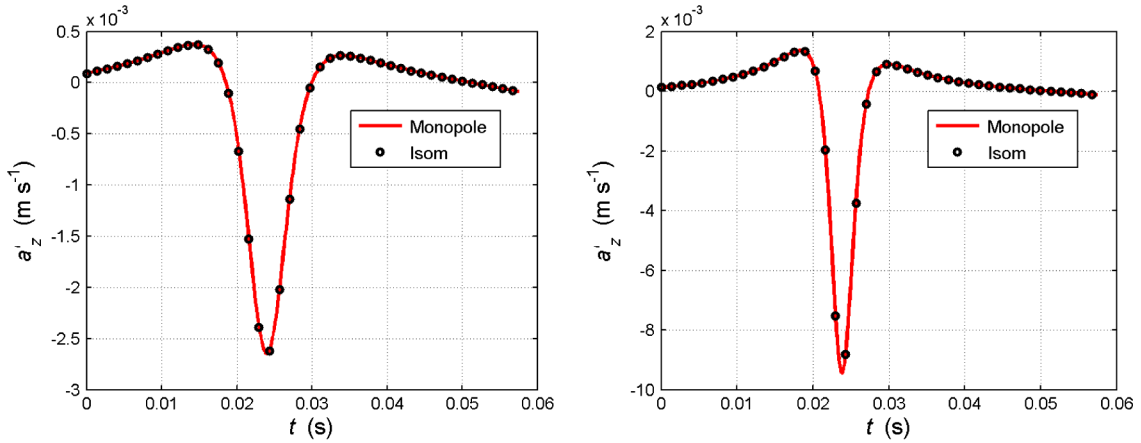

a) b)

Fig. 12 The calculated z-component of acoustic velocity generated by Isom noise source is compared with that of the thickness noise source for different observer positions. a) $\beta = 54$ deg; b) $\beta = 108$ deg.

Table 1 Comparison of computational time is shown for the three test cases used

	Test case 1	Test case 2	Test case 3
Formulation 1A	9.50 s	13.55 s	14.38 s
Formulation V1A	9.52 s	13.58 s	14.41 s

shows the comparison of computational time between formulation 1A and formulation V1A. As can be seen, formulation V1A required the same computation time as formulation 1A for each test case. There is a negligible overhead due to time integration term in the loading part of formulation V1A.

V. Conclusions

In this paper, new formulations are derived for the prediction of the acoustic velocity field generated by moving bodies in a medium at rest. They have been named formulation V1 and V1A, which provide a solution for the acoustic velocity components in the time domain, when the geometry, displacement, and aerodynamic loading of the data surface enclosing the moving body are given. It was shown that the formulations are simple and compact, and they are easy to implement in any of the numerical acoustic pressure codes based on a Green's function solution. It was also observed that formulation V1A uses only the quantities of formulation 1A, requiring the same amount of computation time as formulation 1A. The advantages of formulation 1A over formulations G1 and G1A were demonstrated.

A verification study was conducted based on three cases: a pulsating sphere, a three-dimensional dipole source, and a consistency test for a conventional helicopter rotor case. For the third case, by using a rigid data surface the acoustic velocity field of the thickness noise was compared with that of the loading noise. For the pulsating sphere and the dipole source, by using a permeable data surface the comparison was performed between analytical and numerical solutions. Numerical tests have shown that formulations developed are valid for both rigid and permeable type data surfaces and predict the acoustic velocity accurately.

References

[1] Mao, Y., and Qi, D., "Computation of Rotating Blade Noise Scattered by a Centrifugal Volute," *Proceedings of the Institution of Mechanical Engineers, Part A: Journal of Power and Energy*, Vol. 223, No. 8, 2009, pp. 965–972. doi:10.1243/09576509JPE794

[2] McAlpine, A., Astley, R., Hii, V., Baker, N., and Kempton, A., "Acoustic Scattering by an Axially-Segmented Turbofan Inlet Duct Liner at Supersonic Fan Speeds," *Journal of Sound and Vibration*, Vol. 294, Nos. 4–5, 2006, pp. 780–806. doi:10.1016/j.jsv.2005.12.039

[3] Myers, M. K., and Hausmann, J. S., "Computation of Acoustic Scattering From a Moving Rigid Surface," *Journal of the Acoustical Society of America*, Vol. 91, No. 5, 1992, pp. 2594–2605. doi:10.1121/1.402996

[4] Dunn, M. H., and Tinetti, A. F., "Aeroacoustic Scattering Via The Equivalent Source Method," AIAA Paper 2004-2937, 2004.

[5] Censor, D., "Broadband Scattering From Shear Flows and the Non-Doppler Remote Sensing of Velocity Profiles," *Journal of Sound and Vibration*, Vol. 138, No. 3, 1990, pp. 405–420. doi:10.1016/0022-460X(90)90595-Q

[6] Lee, S., Brentner, K. S., Farassat, F., and Morris, P. J., "Analytic Formulation and Numerical Implementation of an Acoustic Pressure Gradient Prediction," *Journal of Sound and Vibration*, Vol. 319, Nos. 3–5, 2009, pp. 1200–1221. doi:10.1016/j.jsv.2008.06.028

[7] Ffowcs Williams, J. E., and Hawkings, D. L., "Sound Generation by Turbulence and Surfaces in Arbitrary Motion," *Philosophical Transactions of the Royal Society A*, Vol. 264, No. 1151, 1969, pp. 321–342. doi:10.1098/rsta

[8] Farassat, F., "Linear Acoustic Formulas for Calculation of Rotating Blade Noise," *AIAA Journal*, Vol. 19, No. 9, 1981, pp. 1122–1130. doi:10.2514/3.60051

[9] Farassat, F., "Derivation of Formulations 1 and 1A of Farassat," NASA TM-2007-214853, 2007.

[10] Farassat, F., and Succi, G. P., "The Prediction of Helicopter Discrete Frequency Noise," *Vertica*, Vol. 7, No. 4, 1983, pp. 309–320.

[11] Brentner, K. S., "Prediction of Helicopter Rotor Discrete Frequency Noise," NASA TM-1986- 87721, 1986.

[12] Isom, M. P., "The Theory of Sound Radiated by a Hovering Transonic Helicopter Blade," *Polytechnic Institute of New York Report*, Vol. 75, No. 4, 1975.

[13] Farassat, F., "Isom Thickness Noise Formula for Rotating Blades with Finite Thickness at the Tip," *Journal of Sound and Vibration*, Vol. 72, No. 4, 1980, pp. 550–553. doi:10.1016/0022-460X(80)90366-1

[14] Farassat, F., "Extension of Isom's Thickness Noise Formula to the Near Field," *Journal of Sound and Vibration*, Vol. 67, No. 2, 1979, pp. 280–281. doi:10.1016/0022-460X(79)90492-9

[15] Brentner, K. S., and Farassat, F., "Modeling Aerodynamically Generated Sound of Helicopter Rotors," *Progress in Aerospace Sciences*, Vol. 39, No. 2, 2003, pp. 83–120. doi:10.1016/S0376-0421(02)00068-4

[16] Ghorbaniasl, G., and Hirsch, C., "Validation of a Time Domain Formulation for Propeller Noise Prediction," *International Journal of Aeroacoustics*, Vol. 5, No. 4, 2006, pp. 295–301. doi:10.1260/147547206779379895

[17] Fedala, D., Kouidrib, S., and Rey, R., "Numerical Study of Time Domain Analogy Applied to Noise Prediction from Rotating Blades," *Journal of Sound and Vibration*, Vol. 321, Nos. 3–5, 2009, pp. 662–679. doi:10.1016/j.jsv.2008.10.015

A. Lyrintzis
Associate Editor